An investigation of a mixer-ejector nozzle for jet noise reduction

K.B.M.Q. Zaman[1], J.E. Bridges [2], R.S. Castner[3] and A.F. Fagan[4]
NASA Glenn Research Center
Cleveland, OH 44135

Abstract

An experimental study is conducted assessing the performance of an ejector together with an 8:1 aspect ratio rectangular nozzle with the eventual goal of noise reduction for jet engines. Wall static pressure and Pitot probe surveys are conducted to evaluate the performance of the ejector, and sound pressure level measurements are made to assess the impact on noise radiation. It is found that addition of vortex generating tabs at the lip of the nozzle causes large increases in secondary flow entrainment. The baseline ejector (without tabs) often encounters flow resonance with accompanying tones. The tabs have the additional benefit of eliminating those tones. In most cases tried so far, pockets of high-speed fluid remain unmixed. Since jet noise scales as velocity to the eighth power, such 'hot spots' defeat the noise reduction goal. In some cases, there is a reduction in noise amplitudes in the mid-frequency range (5-30 kHz), however, an increase occurs on the low frequency end apparently due to flow unsteadiness. This together with a high frequency noise increase caused by the tabs results in minimal reductions in the overall sound pressure level. The focus of ongoing and future efforts is to achieve sufficient mixing and desirable noise reduction while keeping the hardware short and lightweight.

1. Introduction

The ejector concept has been around for over a century. It is a device that involves a shroud around a primary jet in which secondary or ambient fluid is entrained. The mass flow rate at the ejector exit is increased with a corresponding decrease in the velocity relative to those of the primary jet alone. Turbulent mixing in the shear layer between the primary and secondary streams causes the entrainment and the efficiency of the device depends on the mixing process which in turn depends on geometric as well as flow parameters. Use of mixing devices, such as, lobed mixers on the primary nozzle lip can significantly improve the entrainment process. Configurations involving such mixers have been typically referred to as 'mixer ejector nozzles'.

There have been numerous previous studies on ejectors as fluidic pumps and as a device for thrust augmentation. The vast literature on the subject may be appreciated from the fact that Ref. [1], published in 1967, cited 585 prior publications, dating as far back as 1919. Several of the earliest publications originated from Germany addressing use of steam jets in air pump apparatus applied to ship ventilation. A significant number of publications in the late 20th century focused on analysis of ejector performance. Thrust augmentation and its application in Vertical/Short Takeoff and Landing (V/STOL) aircraft was addressed in many later papers, (e.g., [2-4] and several prior work cited in [1]). More recent publications continued to address aspects of ejector flow theoretically as well as experimentally, e.g., [5-12]. Other investigations addressed application of the ejector technology and methods for improving its performance, e.g., [13-16]. The list of citations given

---

[1] Inlets & Nozzles Branch, AIAA Associate Fellow.
[2] Acoustics Branch, AIAA Associate Fellow.
[3] Inlets & Nozzles Branch, AIAA Associate Fellow.
[4] Optics & Photonics Branch, AIAA Associate Fellow.

herein is far from complete and an interested researcher may look up the bibliographies of the cited papers.

While the phenomenon of thrust augmentation by ejectors is attractive and applies to cases like V/STOL engines, where high lift is desired during takeoff and landing, in other flight applications it is not feasible. This is because with forward flight thrust augmentation diminishes due to increased ram drag. Reference [8] finds that thrust augmentation decreases with increasing flight speed and becomes zero at a Mach number of about 0.7. On the other hand, the ejector principle has been used successfully in a variety of applications, especially for mass flow augmentation. For example, it has been utilized for powering the ‘free-jet’ co-flow in a large-scale jet noise measurement facility at NASA Glenn Research Center (GRC), [17].

Ejectors hold significant potential for jet noise reduction, an aspect that has also been addressed in many previous studies over several decades, e.g., [18-26]. The noise reduction potential stems from the fact that jet noise roughly scales as the eighth power of the exhaust velocity. A decrease in exhaust velocity by using an ejector would thus yield significant reduction in jet noise. As an example, assume that the velocity is reduced to 70% of the primary jet velocity with an ejector shroud that has an exit diameter 1.464 times the primary nozzle diameter (assuming 50% entrainment and uniform flow at the ejector exit, to satisfy continuity). Then from the principle $I \sim U_j^8 D^2$ (where, I is noise intensity, U_j the jet exhaust velocity and D the ejector exit diameter, and assuming a fixed observer distance), about 9 dB reduction in I may be expected. The benefit would increase rapidly with decreasing exhaust velocity. In fact, a reduction in exhaust velocity by mixing fan flow with the primary flow is also the basis for noise reduction achieved with high bypass ratio engines in modern subsonic aircraft.

For noise reduction, the ejector principle was adopted in the design of a high speed civil transport (HSCT) considered in a NASA/Industry High Speed Research (HSR) program conducted during the 1990’s. By using ejectors with various lobed-mixers, exhaust velocities less than 60% of the primary jet velocity were achieved [24]. For example, with a primary-to-ejector area ratio of 2.8 and a lobed-mixer, exhaust velocities were reduced from about 2400 ft/s to about 1400 ft/s. This yielded a reduction in noise intensities by about 15 dB, as measured at various polar locations (and roughly following the simple scaling law discussed in the previous paragraph). The resultant noise, in effective perceived noise level (EPNL) metric, satisfied strict airport noise regulation standards [24]. (FAR36 stage III levels were satisfied with margin; an interested reader may look up [27] for the definitions of noise standards.)

The ejector nozzle in the HSR program turned out to be large and heavy. This is a limitation with the ejector design. Even though much work has been done to improve mixer-ejector nozzle performance [e.g., 12, 14, 16, 18], there is a need for further research to achieve more efficient mixing of the streams so that the hardware can be kept short and lightweight. To that end a fundamental study was initiated at NASA Glenn Research Center (GRC). Initially the effort was focused on the feasibility of a one-sided ejector that might be applicable to aircraft concepts with over-the-wing engine configurations. These concepts often involve an ‘aft deck’ for shielding some exhaust noise from reaching an observer on the ground. If the engine exhaust is rectangular, it could be a relatively simple task of deploying flaps over the exhaust and on the sides to create the one-sided ejector configuration. The effort was exploratory and fundamental in nature and employed an already available 8:1 aspect ratio rectangular nozzle for the primary jet. A suitable ejector box was fabricated that could be attached at the exit of the nozzle. Surveys were made with the main focus on ejector pumping characteristics. Limited data were also obtained on noise radiation characteristics. The scope of this effort, preliminary results, as well as limitations encountered during its course have been discussed in a NASA Technical Memorandum [28]. Those earlier results and results from additional investigation of the one-sided ejector are discussed first in this paper.

Within the parametric space considered in the initial effort, only meagre noise reductions were noted. This is because the flow, while getting mixed on the upper half (side where secondary air was entrained), remained unmixed on the lower half (closed side) of the ejector. The velocities at the ejector exit essentially remained unchanged in the lower half relative to the exit velocities of the primary nozzle. Thus, due to the 8^{th}-power law in velocity-noise relationship there was essentially no noise reduction. At this point the ejector hardware was modified to allow entrainment of secondary air also from the bottom side. The flow in this two-sided ejector was expected to mix better yielding better noise reduction. Only limited explorations could be made so far with the two-sided case and unfortunately significant noise reduction still remains elusive. The results and the status of the entire effort conducted so far are summarized in the following.

2. Experimental Facility

The experiments are conducted in an open jet facility at NASA GRC; [29]. A picture of the nozzle with the one-sided ejector is shown in Fig. 1(a). Figure 1(b) shows a scaled drawing with dimensions in inches. The nozzle has the exit dimensions of 5.34”x0.66”, thus, an equivalent diameter D= 2.12”. The lower plate of the ejector box is placed flush with the lower lip (longer side) of the nozzle. The upper plate (‘ejector flap’, Fig. 1b) is moveable. The side plates have slots allowing placement of the upper plate at different height, H, as well as different inclination angle. The angle α of the upper plate is defined with respect to the axial direction, a positive α denoting the divergent condition. The adjustment of H as well as α is facilitated by sets of ‘plugs’ (Fig. 1a) that are precision made using 3-D printing. The upper plate rests on the four plugs (two on each of the two side plates) and is secured by screws. The plugs also fill the slots on the side walls so that there is no flow leakage.

The shape of the leading edge (LE) of the upper plate, chosen arbitrarily, turned out to be close to optimum for ejector pumping based upon a CFD study on the effect of the LE radius. Details of the CFD study have been described in a paper at the SciTech2019 conference [30]. There are five static pressure ports on the upper plate, located at axial distances of 0.60”, 1.00”, 1.34”, 1.76” and 2.32” from the LE (Fig. 1c). In the experiments, static pressure (P_s) data for all five ports are recorded as a function of the primary jet Mach number. A higher value of the suction pressure (i.e., negative P_s) implies higher entrainment by the ejector.

Data are obtained with and without ‘mixing tabs’ attached to the upper lip of the primary nozzle (Fig. 1d). Each triangular tab has 0.416” base and 0.315” length. There are 11 full and two half tabs at the ends. The tabs penetrate the primary flow at approximately 20° angle. Figure 1(d) shows a configuration where vortex generators (VG’s) on the ejector floor are used in addition to the tabs; the VG’s are described further with corresponding results.

The one-sided configuration was later modified to create the two-sided ejector (Fig. 2). Two new side plates were fabricated having slots to adjust the heights of both the upper and the lower plates (Fig. 2a). Plugs of appropriate heights were again used to set the heights as well as seal the flow. Two tab strips (having the same geometry as described earlier) were used on the upper and the lower lips. In addition, a single tab was also placed on each end of the nozzle. The tab configuration with the ejector removed is shown in Fig. 2(b). A schematic is shown in Fig. 2(c) and further details and notations are described with the results in section 3.2.

A Pitot probe rake is used for Mach number surveys at the ejector exit. These data are integrated to obtain the total mass flow rate through the ejector (m_E). The primary mass flow rate (m_I) is measured by an orificemeter in the supply line. Sound pressure level (SPL) spectra data are obtained using microphones held fixed on an overhead arm. The 'jet Mach number' M_j is defined simply based on the plenum pressure, p_0, and the ambient pressure, p_a, and given by, $M_j = (((p_0/p_a)^{(\gamma-1)/\gamma} - 1)\frac{2}{\gamma-1})^{1/2}$, where γ is the ratio of specific heats for air.

3. Results

3.1 One-sided ejector: The results for the one-sided ejector are presented first. Static pressure (P_s) measured as a function of M_j at the five ports is shown in Fig. 3 for a height H=0.902", as an example, with and without the tabs. Note that the parameters G and H are related directly (Fig. 1b); H will be quoted in the discussions while corresponding values of G are given for several cases in the figures. A comparison of the data for the no-tab case (a) and the tab case (b) shows that the tabs have increased the suction pressure, more than 3-fold on the high end of the M_j-range. The tabs cause increased mixing, so more ambient air is entrained, resulting in higher suction pressures. The divergence angle of the upper plate is also found to have a large impact on the suction pressure. This is shown in Fig. 4 with data for four different values of α (0°, 2°, 4° and 6°). All data here are with the tabs. One finds that the 'peak' suction pressure increases sharply (by another 3-fold) when a divergence is introduced. The maximum is reached in the α range of 2° to 4° (port 1 pressure reaching about -9 psig). At even higher values of α there is a drop-off due to flow separation on the upper wall, that becomes clear from Pitot survey data shown next.

Pitot probe survey data are obtained at the exit of the ejector and contours of Mach number are presented. The relative location of the ejector exit is outlined by dashed lines in all contour plots. In Fig. 5, the effect of ejector height H, with and without the tabs, is captured. For the no-tab case (left column), flow separation occurs around the middle of the upper surface. The separated zone becomes clearer at H=1.05" and the flow is completely separated at H=1.33". With the tabs (right column) the flow is completely attached on the upper surface at H=1.05" and only partially separated at H=1.33". These results are commensurate with the higher suction pressures measured with the tab cases.

Similar comments can be made about the effect of upper plate divergence from the data in Fig. 6. For α=2°, the flow is completely attached on the upper surface. At α=4° some flow separation has taken place while at α=6° the separation is extensive. These results explain why the suction pressure attains a maximum value in the α range of 2° to 4°.

Mass flux results obtained by integration of the Pitot survey data are shown in Fig. 7. The effect of tabs is shown in Fig. 7(a). Clearly, the mass flux is increased by the tabs at all values of H. A maximum flux is obtained around H= 1.33". The entrainment characteristics are shown in Fig. 7(b). The primary jet mass flow rate (m_I) is shown on the top. With increasing H a decrease in m_I is noted, apparently due to static pressure changes caused by the ejector. Combining these data with the total mass flow rate (m_E) the entrainment rate is obtained as shown at the bottom of Fig. 7(b). A maximum entrainment ratio of about 34% occurs around H=1.33".

Figure 8 compares sound pressure level (SPL) spectra with and without tabs for 4 different values of H. Pairs of traces are shown in each figure for no-tab (blue) and tab (red) cases. It is apparent that the bare nozzle together with the ejector often yields resonant tones. Addition of the tabs not only eliminates the tones but also brings down the broadband levels. With the presence of the tones there is 'broadband noise amplification' ([31, 32]). Thus, elimination of the tones also causes a drop in the broadband levels. In Fig. 9, data for a convergent case (α=-3°) as well as a divergent case (α=+3°) are shown with and without tabs. In both cases the flow without tabs involves tones. The tabs again effectively suppress the tones and reduce broadband noise levels.

So, the main inference so far is that the tabs make a large increase in the suction pressure. A further significant increase is obtained with a small divergence of the upper plate. An increase in suction pressure implies an increased pumping and this is corroborated by the Mach number contours at the exit of the ejector. The baseline ejector often involves resonant tones. This, of course, would be unacceptable in practice. Fortunately, the tabs completely eliminate these tones in all the cases tested. Not only the tones are eliminated but with that the associated 'broadband noise amplification' is also suppressed causing a large drop in the broadband levels.

Unfortunately, the primary goal of noise reduction is not met with the one-sided configuration explored so far. In Fig. 10, the spectral data are shown for three cases: the free jet from the nozzle without the ejector or tabs (red curve), free jet from the nozzle fitted with the tabs (blue curve), and for the ejector configuration with the tabbed primary nozzle having H=0.902" (green curve). These data are shown for two polar locations as indicated. These are also shown in log scale for the abscissa in order to clearly illustrate the changes on both the low and high frequency ends. (Note that data for the ejector without tabs case are not shown in Fig. 10. The broadband levels for that case, involving the tones (Fig. 8b), would be much higher.) Addition of tabs has caused an increase in the high frequency energy but there is a perceptible reduction in low frequency energy (compare red and green curves). The addition of the ejector, however, has made little further difference (compare green and blue curves). The OASPL values (3^{rd} column in legend) have not reduced significantly.

The reason for the lack of noise reduction with the present ejector becomes clear from the Mach number data shown in Figs. 5 and 6. It can be seen that in all cases there is a layer of high-speed flow on the lower half of the cross-sectional plane. The flow in that region has the same velocity as that at the exit of the primary nozzle. Thus, while enhanced mixing has been achieved by the tabs in the upper half of the ejector, the flow underneath has not mixed. Even a small "hot spot" (i.e., high velocity flow) would defeat the goal of noise reduction via the $I{\sim}U_j^8$ scaling law. As recognized much earlier [18], "maximum velocity at the ejector exit is the most important parameter in the noise generation". Thus, essentially no noise reduction has been achieved with the configuration tested.

In an attempt to mix the flow on the lower half, vortex generators were used on the floor of the ejector. Figure 11 shows an example of the results. On top left (Fig. 11a) is the Mach number distribution for the tabbed case as in Fig. 5. The corresponding plot for the case with 6 vortex generators on the floor (Fig. 1c), in addition to the tabs, is shown on bottom left. (The VG's are 3-D printed triangular 'ramps' with 0.4" base and 0.2" height at the downstream apex; see inset in Fig. 1d). A comparison shows only minor improvement in mixing has occurred. The two plots on the right of Fig. 11 represent corresponding data obtained with a longer ejector ($L=L0+\Delta L$=6", Fig. 1a). (With the extended length, the survey had to be conducted somewhat farther downstream from the exit in order to clear the screw heads fastening the extensions. However, measurements at two stations, x=0.04" and 0.24", for a given case showed practically imperceptible changes in the contour plots as well as in the integral quantities as described later.) With the extension, some further improvement in mixing has taken place. However, flow at the bottom half is still unmixed. Noise data (not shown) indicated only a small reduction in OASPL with the VG's.

3.2 Explorations with the two-sided ejector: At this point it appeared that some secondary flow must be admitted from the bottom of the ejector to achieve the desired mixing. This is explored with some modification of the hardware. The modification involved two new side plates (Fig. 2a) and a 3-D printed LE section attached to the bottom plate (Fig. 2c). Note that this arrangement left an asymmetry in the 'throat' location between the upper and lower sides. Two ejector configurations have been tried: 'EJ1' has entrance gap (*G*) of about 0.3" on both the upper and the lower sides; the plate-to-plate (parallel) height (*H*) being about 1.32". The second configuration 'EJ2' has $G \approx 0.17$" on the upper side and $G \approx 0.175$" on the lower side with $H \approx 1.06$". The gaps and the heights are set by suitable plugs on both lower and upper slots of the side plates (Fig. 2a). Also two tab configurations are tried: 'TB1' is the same as tried for the one-sided case. The tabs in this case, applied on both upper and lower lips, have approximate penetration of 20° into the primary flow. In the second tab configuration, 'TB2', the tabs are bent so as to have approximately 30° penetration. With both TB1 and TB2, a single tab is applied on each end (short side) of the nozzle, as can be seen in Fig. 2(b). The end tabs have a base width of 0.5" and approximately 45° penetration into the flow; the angle at the tip is 90°.

Pitot survey results are shown in Fig. 12, as examples. In Fig. 12(a) data for the baseline nozzle without tabs or the ejector is shown. A uniform core flow is seen. Small deviations on the edges are due to thin boundary layers and coarse spatial resolution in the survey. In 12(b), corresponding data for the tab configuration TB2 (without ejector) is shown. The 'footprint' of the tabs are visible. Here the tabs are bent roughly to have 30° penetration; small differences from tab to tab resulted in a non-uniform spacing of the high-speed 'tongues' on the edges. In 12(c) data for the no-tab case with EJ1 are shown. An upward deflection of the core flow is noted which is due to the asymmetry in the upper and lower plate 'throat' locations (Fig. 2c). The effect of the tab configuration TB2 with the ejector configuration EJ2 is shown in Fig. 12(d). An upward deflection of the core flow is again noted due to the asymmetry in the plate geometries. A better mixing has been achieved relative to the one-sided cases, however, still there are 'hot spots'.

Limited measurements were made for the entrainment characteristics. The results are shown in Table 1. These data are for constant plenum pressure of about 10 psig. The tabs used (TB2) are large and aggressive in order to mix the flow, thus, there is large blockage. Comparing data in rows 1 and 2 of table 1 it can be seen that TB2 has caused about 17% flow blockage. For ejector performance, of interest is the entrainment fraction shown in the last column of table 1. Use of TB2 has caused the entrainment to increase from 23.6% to 47.1% (rows 3 and 4). Note that this is significantly larger than corresponding values obtained with the one-sided ejector (maximum of 34%, Fig. 7b). Addition of the 2" extension has not increased the entrainment fraction any more although, as it will become clear shortly, the flow gets a chance to mix better. With ejector EJ2 (with smaller gap, $G \approx 0.17$") the entrainment is not as much, as seen from the values in rows 6-8 of table 1. The last row of data is added to demonstrate that the slight difference in the measurement location (x=0.24" versus x=0.04") did not make noticeable difference in the flux values (compare with data in row 6).

Table 1 Entrainment characteristics for 2-sided ejector.

Case	Configuration	Survey location x (in)	Ejector length, L (in)	Exit mass flux Pitot, m_E (lb/s)	Primary mass flux orificemeter, m_I (lb/s)	Entrainment fraction, $(m_E - m_I)/m_I$
1	NTB NEJ	--	--	--	2.0200	--
2	TB2 NEJ	--	--	--	1.676	--
3	No tab EJ1	0.040	3	2.5207	2.0395	0.236
4	TB2 EJ1	0.040	3	2.4764	1.6830	0.471
5	TB2 EJ1	0.240	5	2.4583	1.6920	0.453
6	TB2 EJ2	0.040	3	2.2455	1.7240	0.303
7	TB2 EJ2	0.240	5	2.2164	1.7560	0.262
8	TB2 EJ2	0.240	3	2.2335	1.7240	0.296

In Figs. 13-17, Pitot survey results and corresponding SPL spectra are shown side by side for several combinations of the ejector and tab configurations. In the spectral plots, comparison is made for a given tab configuration with and without the ejector. This way, the effect of the ejector on noise reduction is directly assessed. Figure 13 shows results for tabs TB1 (20 degree penetration) with and without ejector EJ1 (G=0.3 gaps). There is better mixing relative to the one-sided cases but hot spots are still present in the middle. Noise data exhibit noticeable reduction in amplitudes within a mid-frequency range of about 5-30 kHz. However, there is no decrease in amplitudes on the high as well as on the low frequency end. OASPL has reduced by only 0.6 dB. The poor reduction in OASPL is primarily due to lack of noise reduction on the low frequency end. In fact, in many cases an increase in low frequency amplitudes is noted. The energy is concentrated in weak tone-like peaks, presumably owing to unsteady flow separation within the ejector. Effect of tabs TB2 with EJ1 is shown in Fig. 14. Here, the effect of the ejector is somewhat worse relative to that seen in Fig. 13. There is increase in amplitudes on the low frequency end where multiple peaks are noted. It is likely that these weak tone-like peaks also cause some increase in the broadband levels ('broadband noise amplification' by tones, [31]), resulting in poor overall acoustic performance of the ejector.

Lengthening the ejector shows a benefit. This can be seen in figure 15 where ejector EJ1 has been extended by 2"; (here ejector length to primary nozzle diameter ratio is about 2.35 which is comparable to some of the configurations tested in [18] and [24]). The data may be compared to those shown in Fig. 14. There is better mixing as well as clearer reduction in the spectral amplitudes. The OASPL has reduced by about 1dB. Note that the peak Mach number at the exit (Fig. 15a) is about 0.76. Using the simple scaling law discussed in the Introduction a reduction in OASPL by about 3.7dB is expected but in reality, only 1 dB reduction has taken place. This appears to be primarily due to the low frequency energy increase from the unsteadiness of the flow.

Finally, results for a combination of ejector EJ2 with tabs TB2, with and without the 2" extension, are shown in Figs. 16 and 17. The noise data in Fig. 16 exhibit significant high frequency penalty in addition to the weak tones at low frequencies. The result is a net increase in OASPL. Addition of the 2" extension (Fig. 17) does show better mixing. However, the noise reduction is not as good as seen in Fig. 15 for combination of EJ1, TB2 and the 2" extension. The higher penetration of TB2 (30°) not only caused noise increase on the high frequency end but also presumably led to more flow unsteadiness leading to higher amplitudes on the low frequency end.

Thus, in terms of noise reduction the explorations so far have not produced good results. It is thought that part of the problem is high frequency noise escaping through the inlet as well as the downstream end. Perhaps, the worst offender is the low frequency unsteadiness causing multiple weak tones. Thus, noise is increased not only by the tones themselves but also through broadband noise amplification. This has resulted in poor reduction of OASPL. It should be recognized that only limited parametric variations were made so far with the two-sided ejector. Only one tab geometry has been used albeit with two penetrations. Further explorations are planned with variations in the tab and other mixer geometries. It appears that a better design is needed for the inlet so that less noise escapes from that end. Attention must also be given on flow separation on the ejector walls that apparently led to the low frequency unsteadiness.

Conclusions

A rectangular mixer-ejector nozzle is explored with the ultimate goal of achieving jet noise reduction for various aircraft concepts. In this fundamental exploratory study an 8:1 aspect ratio nozzle is used together with a simple ejector box. Wall static pressure, Pitot probe survey and limited noise measurements are made. These quantities are evaluated as a function of geometric parameters with and without mixing tabs. At first, a one-sided ejector configuration is studied. With increasing velocity of the secondary flow at the inlet gap, static pressures near the inlet decrease. The intensity of this 'suction' pressure thus provides a measure of the secondary flow entrainment and ejector pumping efficiency. As the gap width is varied while keeping the upper and lower surfaces of the ejector parallel, pumping efficiency varies. Highest pumping occurs around gap widths approximately half the nozzle width (short dimension). With further increase in gap width the efficiency decreases rapidly when the flow is no longer attached to the upper surface of the ejector. The tabs are found to increase the suction pressure often by a factor of 3. The tab effect occurs due to enhanced mixing between the nozzle flow and the induced secondary flow. For a given gap, the pumping is found to be enhanced further by the introduction of a divergence of the upper surface. Most efficient pumping is achieved for an α-range of 2°-4° together with the mixing tabs. There is another three-fold increase in the suction pressure with the divergence over that achieved by the tabs in corresponding parallel configuration. The inferences on the pumping efficiencies from the static pressures are generally corroborated by Pitot probe surveys at the exit of the ejector.

Subsequently, the configuration is modified so that ambient air is entrained from both upper and lower sides of the nozzle. Combinations of tab penetration and ejector gap width are explored. While with the one-sided case, a layer of high-speed air remains unmixed on the lower half of the ejector, it is mixed better in the two-sided case. However, with the configurations tried so far 'hot-spots' still have remained in the central region of the cross-section. Extending the length of the ejector improves the mixing. As expected, the net entrainment is found to be significantly larger with the two-sided case compared to the one-sided case.

The baseline ejector without any tabs on the nozzle lip often encounters flow resonance with accompanying tones. This is true for both the one- and the two-sided cases. Use of tabs not only enhances secondary flow entrainment but also eliminates those tones. Thus, use of some mixing devices on the nozzle lip is called for in practical applications.

However, with the tabbed nozzle the addition of the ejector is found to produce insignificant reduction in overall sound pressure levels. With the best mixed flow in the 2-sided case, there is noise reduction in the mid frequency range (5-30kHz). However, there is high frequency noise increase due to the tabs. More serious is an increase in low frequency amplitudes apparently due to unsteadiness in the flow. This contributes largely leading to insignificant reductions in OASPL. Thus, with the configurations tried so far, the jet noise reduction goal has remained elusive.

It should be borne in mind that for a rectangular configuration with lobed mixers the HSR experiments [24] clearly demonstrated noise reductions by the ejector when compared to corresponding conic nozzle data. A similar result was reported for a round configuration with lobed primary nozzle in Ref. [18]. Reference [26] reported results for both 2-D and axisymmetric configurations for variations in several geometrical parameters such as auxiliary doors near the inlet of the ejector. While noise reduction observed in [26] was modest, further reductions were achieved with acoustic liners. These cited experiments employed lobed mixers and relatively long ejector lengths. The question remains if with simpler (and lighter) mixers like the tabs, and shorter ejector lengths, significant noise reduction could be achieved. The present exploration has been limited so far utilizing only one tab geometry with the given nozzle. Future efforts will focus on getting the flow mixed further, using different tab configurations and ejector geometry, so that the exhaust velocities are low uniformly. The emphasis will be on achieving this and the resultant noise reduction while keeping the ejector hardware short and lightweight.

Acknowledgement
The work was in support of NASA's Commercial Supersonic Technologies (CST) Project.

References:

1. Huang, K.P. and Kisielowski, E., "An investigation of the thrust augmentation characteristics of jet ejectors", *USAAVLABS Report 67-8*, Contract DA-44-177-AMC-322(T), U.S. Army Aviation Materiel Laboratories, Fort Eustis, Virginia, April 1967.
2. Quinn, B., "Compact ejector thrust augmentation", *J. Aircraft*, vol 10, no. 8, August, 1973.
3. Bevilaqua, P.N., "Evaluation of hypermixing for thrust augmenting ejectors", *J. Aircraft*, vol. 11, no. 6, p. 348-354, 1974.
4. O'Donnell, R.M. and Squyers, R.A., "V/STOL ejector short diffuser study final report", *ATC Report No. B-94300/6CR-26*, Prepared for Naval Air Development Center, Warminster, PA, June, 1976.
5. Porter, J.L., Squayers, R.A. and Nagaraja, K.S., "An overview of ejector theory", *AIAA Paper 81-1678*, AIAA Aircraft systems and technology conference, Dayton, OH, August 11-13, 1981.
6. Nagaraja, K.S., "Advances in ejector technology – a tribute to Hans von Ohain's vision", *In AFWAL A collection of papers in the Aerospace Sci.*, p. 499-517, NTIS HC A99/MF A01 CSCL 20D, June 1982.
7. Bernal, L.P. and Sarohia, V., "Entrainment and mixing in thrust augmenting ejectors", *AIAA Paper 83-0172*, 21st Aerospace Sciences Meeting, Reno, NV, Jan. 10-13, 1983.
8. Papamoschou, D., "Analysis of partially mixed supersonic ejector", *J. Prop. & Power*, vol. 12, no. 4, p. 736-741, 1996.
9. Heiser, W.H., "Ejector thrust augmentation", *J. Prop. & Power*, vol. 26, no. 6, p. 1325-1329, 2010.
10. Tew, D.E., Teeple, B.S. and Waitz, I.A., "Mixer-ejector noise-suppressor model", J. Prop. And Power, vol. 14, No. 6, pp. 941-950, 1998.
11. Shan, Y., Zhang, J. and Huang, G., "Experimental and numerical studies on lobed ejector exhaust sytem for micro turbojet engine", Engineering Applications of Compuational Fluid Mechanics, 5:1, 141-148, DOI: 10.1080/19942060.2011.11015358, 2011.
12. Liu, F., "Review on ejector efficiencies in various ejector systems", International Refrigeration and air conditioning conference at Purdue, July 14-17, 2014.
13. Throndson, L.W., "Compound ejector thrust augmentor development", *ASME Paper 73-GT-67*, ASME Gas Turbine Conf., Washington D.C., April 8-12, 1973.
14. Presz, W.M. Jr., Morin, B.L. and Gousy, R.G., "Forced mixer lobes in ejector designs", *J. Propulsion*, vol. 4, no. 4, p. 350-355, 1988.
15. Presz, W.M. Jr., Reynolds, G. and McCormick, D., "Thrust augmentation using mixer-ejector-diffuser systems", *AIAA Paper 94-0020*, 32nd Aerospace Sciences Meeting, Reno, NV, January 10-13, 1994.
16. Presz, W.M. Jr., Blinn, R.F. and Morin, B.L., "Short efficient ejector systems", *AIAA Paper 87-1837*, 23rd Joint Propulsion Conference, San Diego, CA, June 29- July 2, 1987.
17. Long, M.J., "Experimental investigation of an ejector-powered free-jet facility", *AIAA Paper 92-3569*, 28th Joint Propulsion Conf., Nashville, TN, July 6-8, 1992. (Also NASA TM 105868).

18. Coles, W.D., Mihaloew, J.A. and Callaghan E.E., “Turbojet emgine noise reduction with mixing nozzle-ejector combinations”, *NACA TN 4317*, August, 1958.
19. Seiner, J.M. and Krejsa, E.A., “Supersonic jet noise and High Speed Civil Transport”, *AIAA paper 89-2358*, 25th Joint Propulsion Conference, Monterey, CA, July 10-12, 1989.
20. Lord, W.K., Jones, C.W., Stern A.M., Head, V.L. and Krejsa, E.A., “Mixer ejector nozzle for jet noise suppression”, *AIAA Paper 90-1909*, 26th Joint Propulsion Conference, Orlando, FL, July 16-18, 1990.
21. Presz, W.M. Jr., “Mixer/ejector noise suppressors”, *AIAA Paper 91-2243*, 27th Joint Propulsion Conference, Sacramento, CA, June 24-26, 1991.
22. DeBonis, J.R., “Full Navier-Stokes analysis of a two-dimensional mixer/ejector nozzle for noise suppression”, *AIAA Paper 92-3570*, 28th Joint Propulsion Conference, Nashville, TN, July 6-8, 1992.
23. Tillman, T.G. and Presz, W.M. Jr., “Thrust characteristics of a supersonic mixer ejector”, *J. Prop. & Power*, vol. 11, no. 5, p. 931-937, 1995.
24. Majjigi, R.K., Balan, C., Mengle, V., Brausch, J.F., Shin, H. and Askew, J.W., “Low noise exhaust nozzle technology development”, *NASA CR 2005-213325*, February, 2005 (originally published as NASA Report HSR044, Nov., 1996).
25. Raman, G. and Taghavi, R., “Aeroacoustic characteristics of a rectangular multi-element supersonic jet mixer-ejector nozzle”, *J. Sound and Vib*., vol. 207, no. 2, p. 227-247, 1997.
26. Krasheninnikov, S.J., Mironov, A.K., Shenkin, A.V. and Zhitenev, V.K., “Mixer-ejector nozzles: acoustic and thrust characteristics”, International J. of Aeroacoustics, vol. 4, No. 3&4, pp. 267-288, 2005.
27. Dickson, N., “ICAO Noise standards”, *International Civil Aviation Organization Symposium on aviation and climate change, “destination green”*, Montreal, Canada, May 14-16, 2013.
28. Zaman, K.B.M.Q., Fagan, A.F., Bridges, J.E., “Experimental investigation of a one-sided ejector nozzle”, NASA/TM—2019-220064, February, 2019.
29. Zaman, K.B.M.Q., Fagan, A.F., Bridges, J.E. and Brown, C.A., “An experimental investigation of resonant interaction of a rectangular jet with a flat plate”, *J. Fluid Mech*., vol. 779, pp. 751-775. doi:10.1017/jfm.2015.453, 2015.
30. Hoter, Z., Castner, R.S. and Zaman, K.B.M.Q., “CFD Optimization of Ejector Flaps in a One-Sided Mixer Ejector Nozzle”, to be presented at the *SciTech2019* conference, January 5-9, 2019, San Diego, CA.
31. Bechert, D. and Pfizenmaier, E., “On the amplification of broadband jet noise by a pure tone excitation”, *J. Sound and Vibration*, 43, pp. 581-587.
32. Zaman, K.B.M.Q., 1985, “Far-field noise of a subsonic jet under controlled excitation”, *J. Fluid Mech., 152*, pp. 83-111.

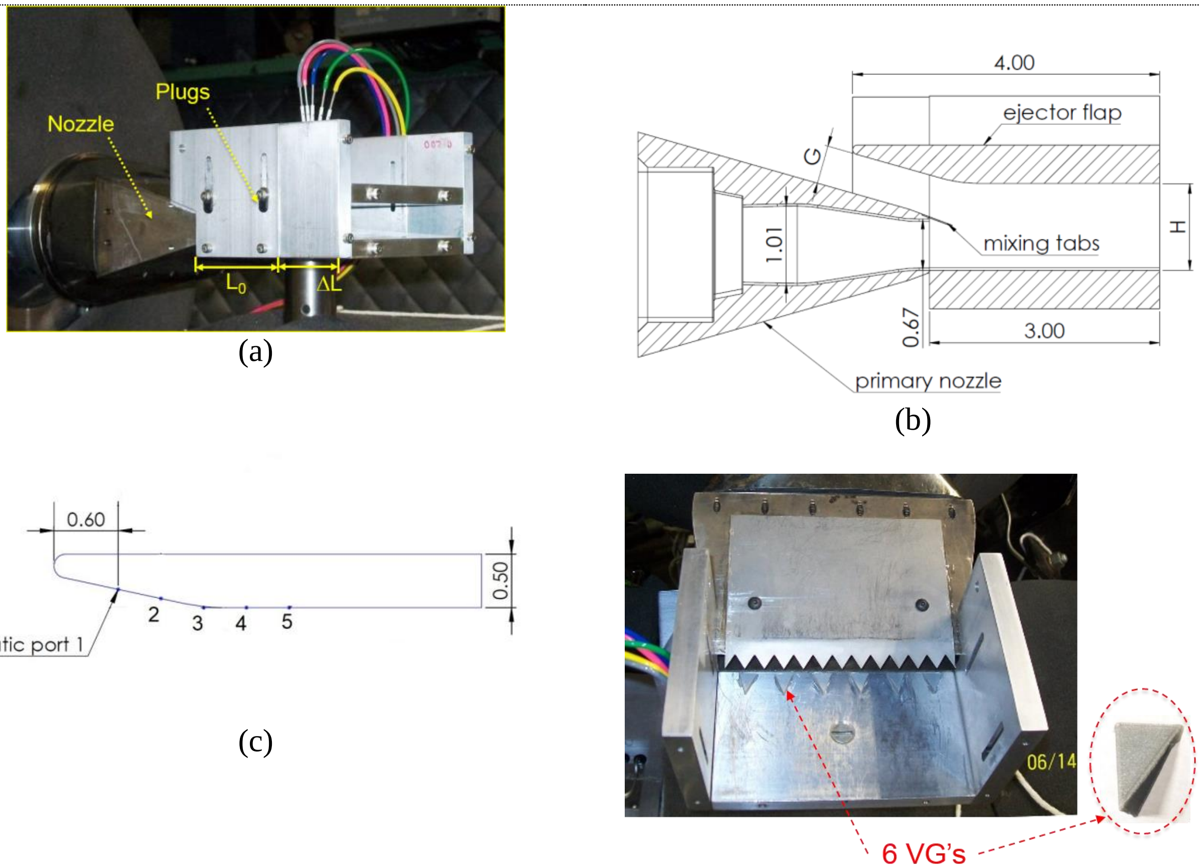

(a) (b) (c) (d)

Fig. 1 One-sided ejector. (a) Picture of 8:1 rectangular nozzle with ejector box, (b) schematic with dimensions in inches, (c) upper plate with static pressure port locations, (d) picture of nozzle with tab strip, also showing 6 VG's on the floor (top plate removed); a single VG is shown in inset.

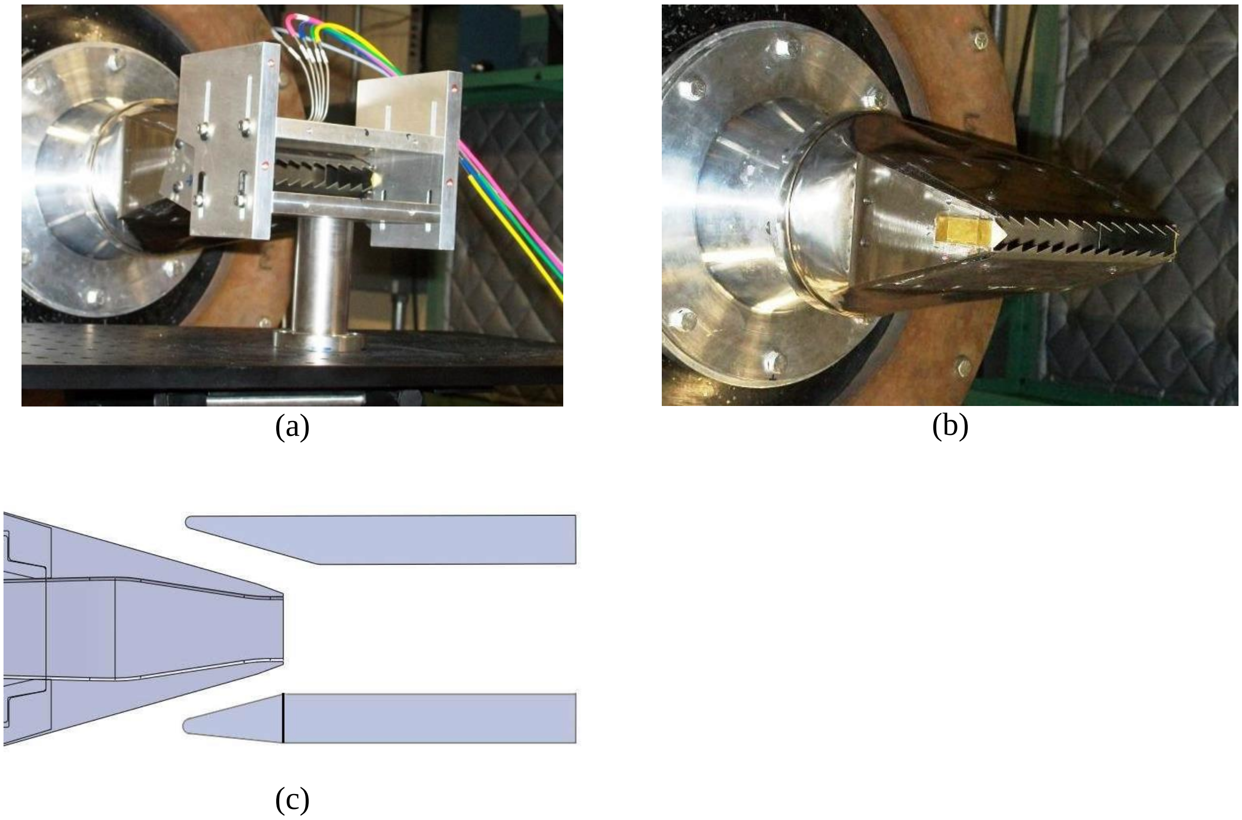

Fig. 2 Two-sided ejector: (a) picture of overall setup, (b) picture of nozzle with tabs on all sides, (c) schematic of configuration.

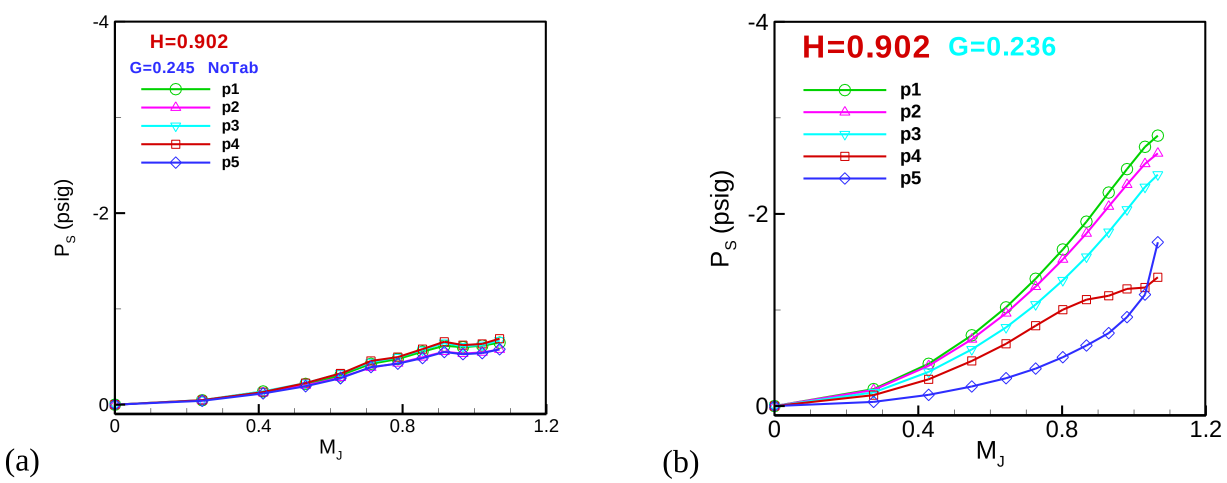

Fig. 3 Static pressure versus M_j for H=0.900 for one-sided case. (a) no-tab case, (b) tabs on nozzle upper lip; each graph has data from the five ports.

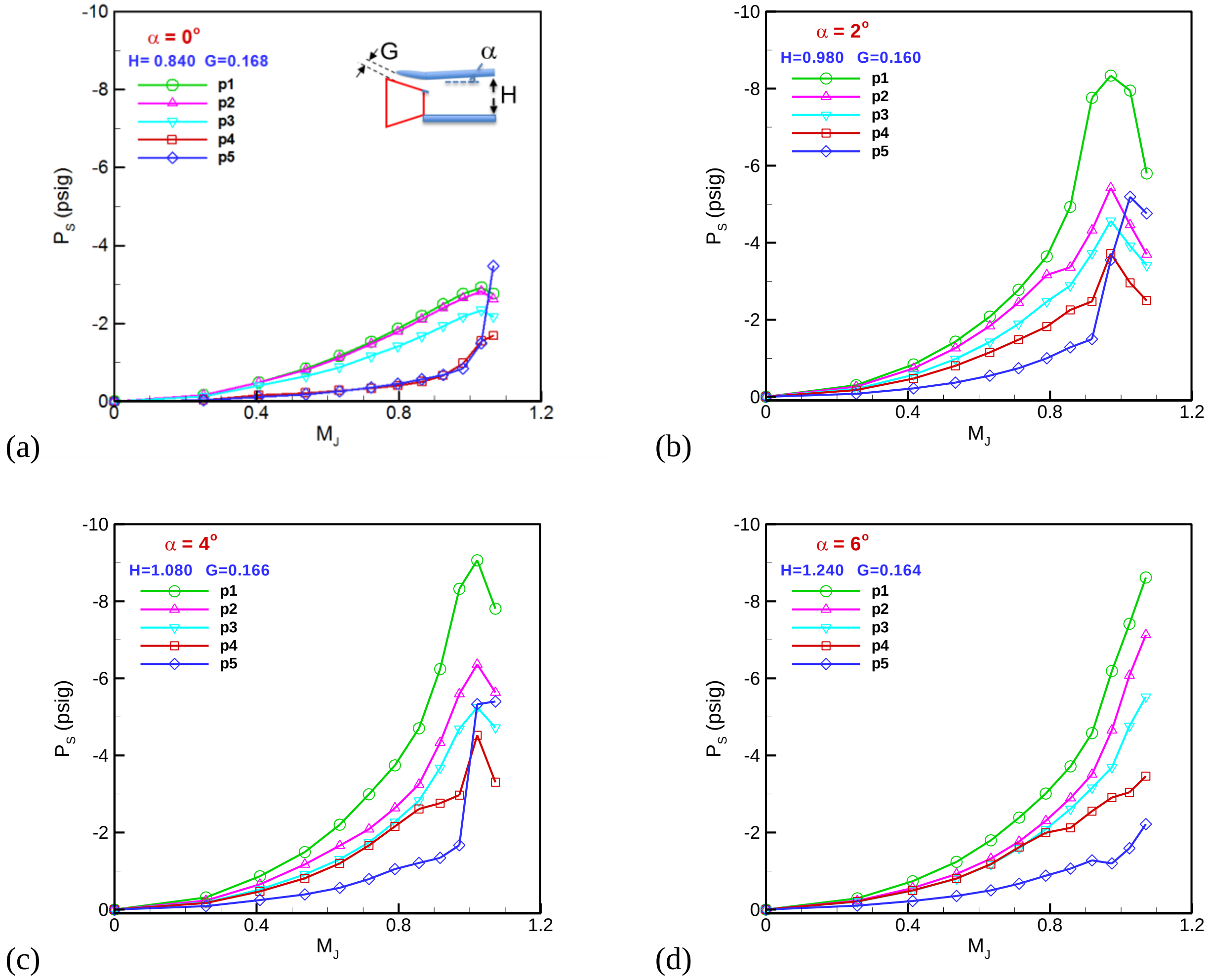

Fig. 4 Static pressure versus M_j for the one-sided case for different divergence angle of the upper plate (α), as indicated; the gap G was approximately held the same.

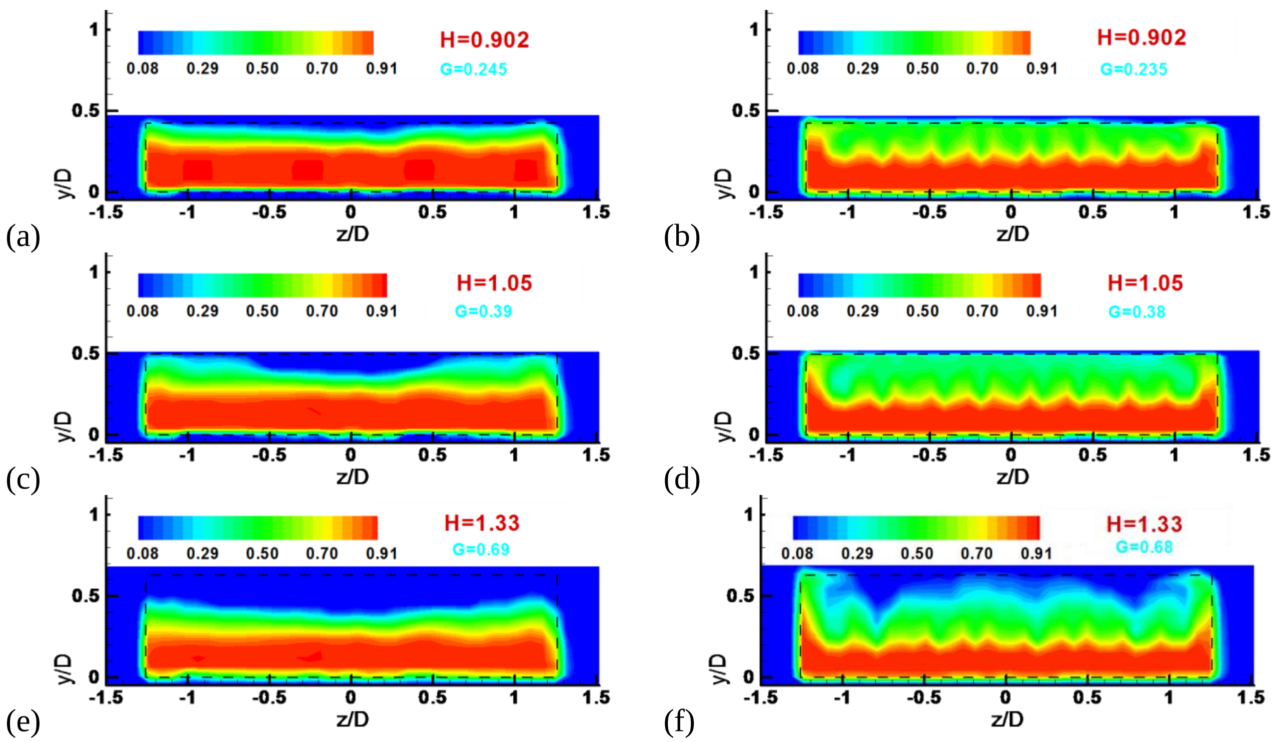

Fig. 5 Mach number contours at exit of one-sided ejector (x=0.04”) for different H, as indicated; M_j =0.9. No tab data in (a), (c) and (e) on left; corresponding tab cases in (b), (d) and (f) on right.

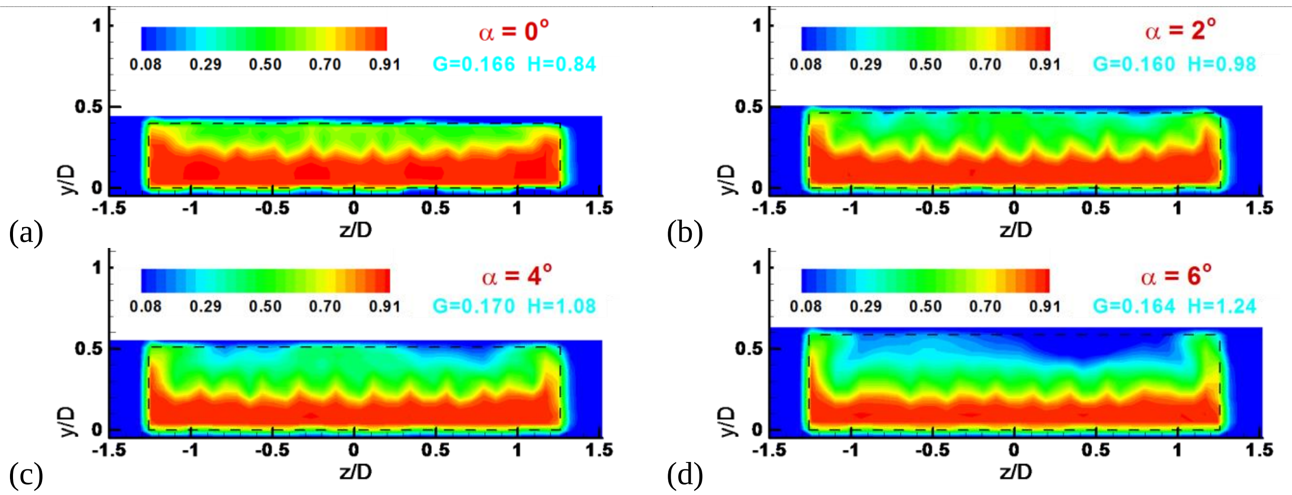

Fig. 6 Mach number contours at exit of one-sided ejector (x=0.040”) for different divergence angle (α), as indicated; M_j =0.9, tab cases.

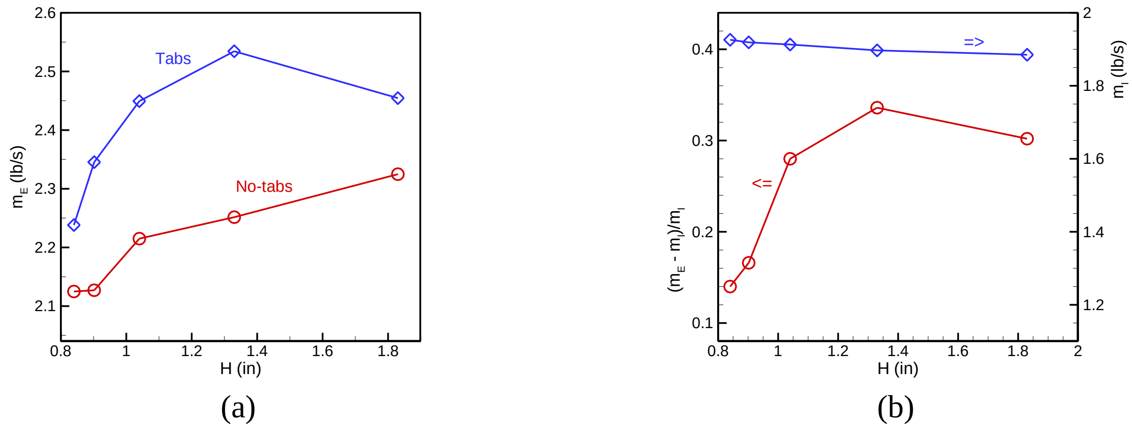

Fig. 7 Mass flow rates for one-sided ejector versus *H*; M_j =0.9. (a) Rates for tabs versus no-tab cases obtained from Pitot survey at ejector exit, (b) primary flow rate and entrainment for the tab case.

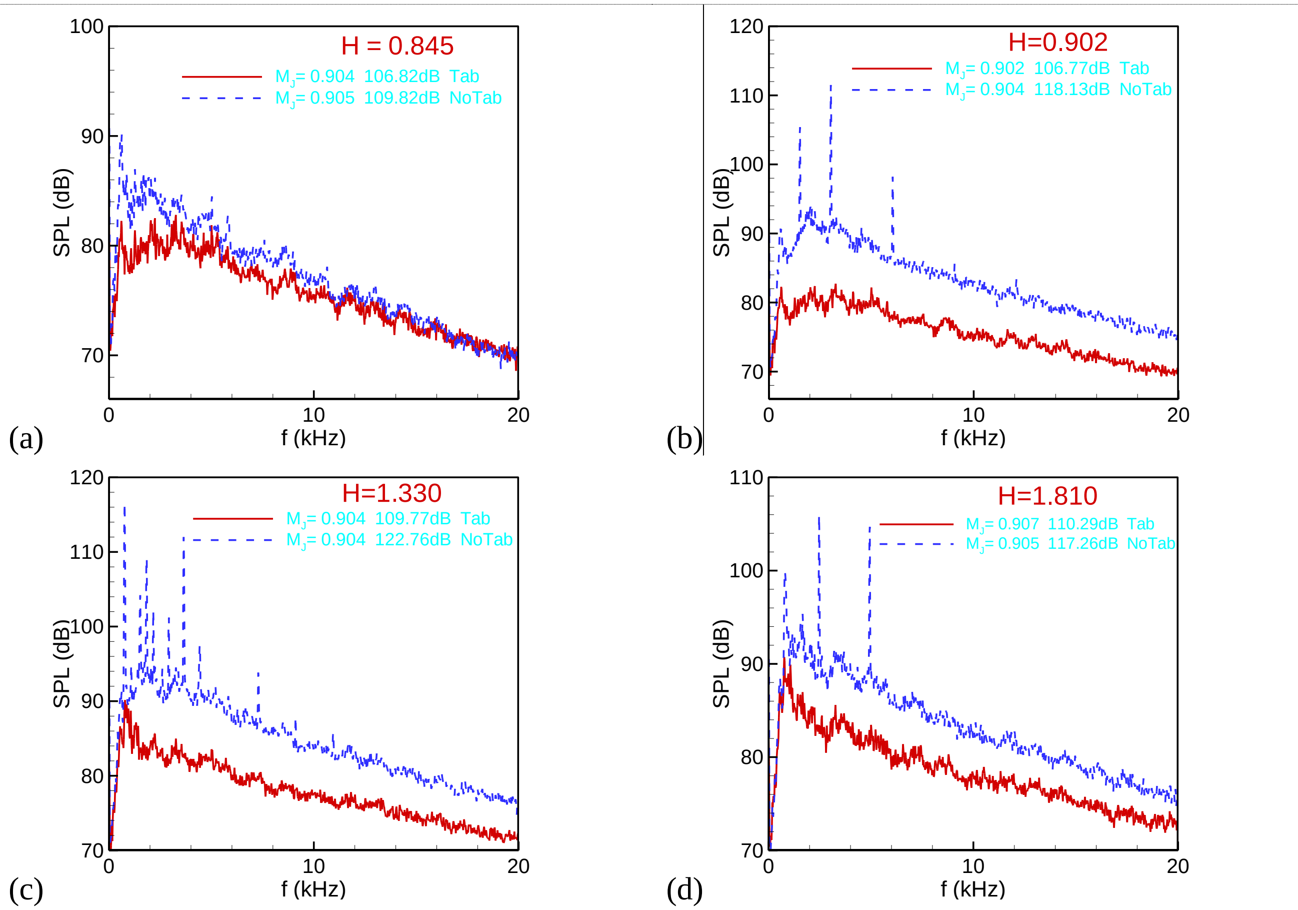

Fig. 8 Sound pressure level (SPL) spectra for one-sided ejector with varying *H*, as indicated; M_j =0.9. In each plot blue curve is for no-tab case and red curve is for tab case.

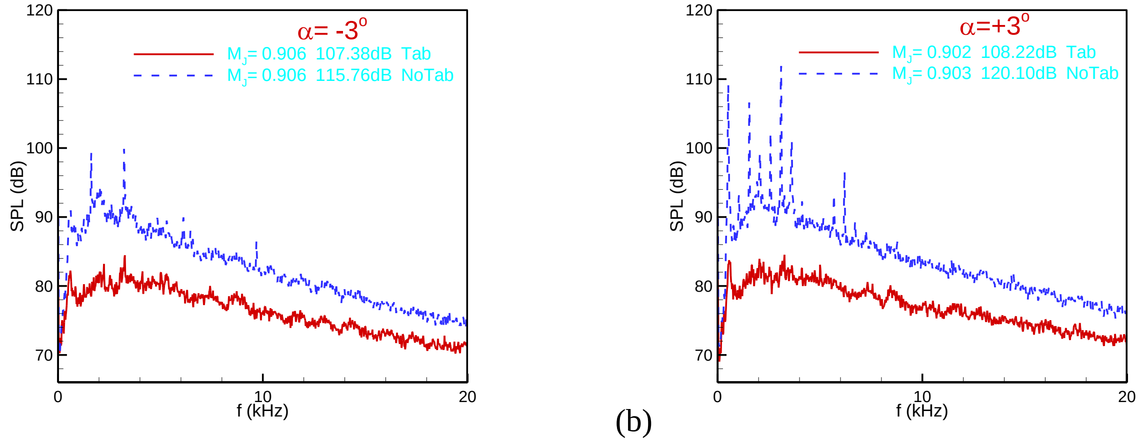

(a) (b)

Fig. 9 SPL spectra for one-sided ejector; M_j =0.9. (a) Convergent case (α= -3°, H=0.883”, G=0.375”), (b) divergent case (α=3°, H=1.03”, G=0.164”).

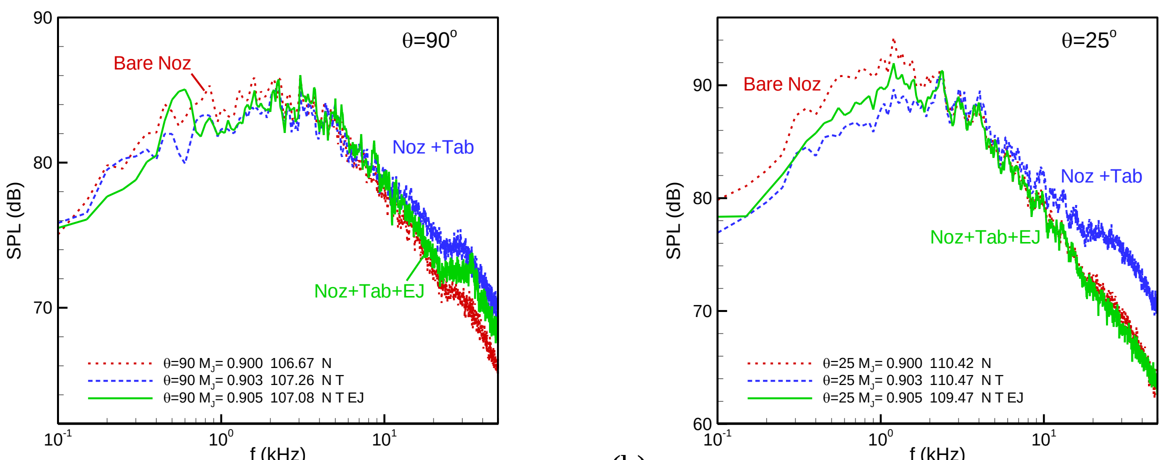

(a) (b)

Fig. 10 SPL spectra for one-sided ejector at M_j =0.9 at two polar locations; red: bare nozzle, blue: nozzle fitted with tabs without ejector, green: nozzle with tabs and ejector (H=0.900).

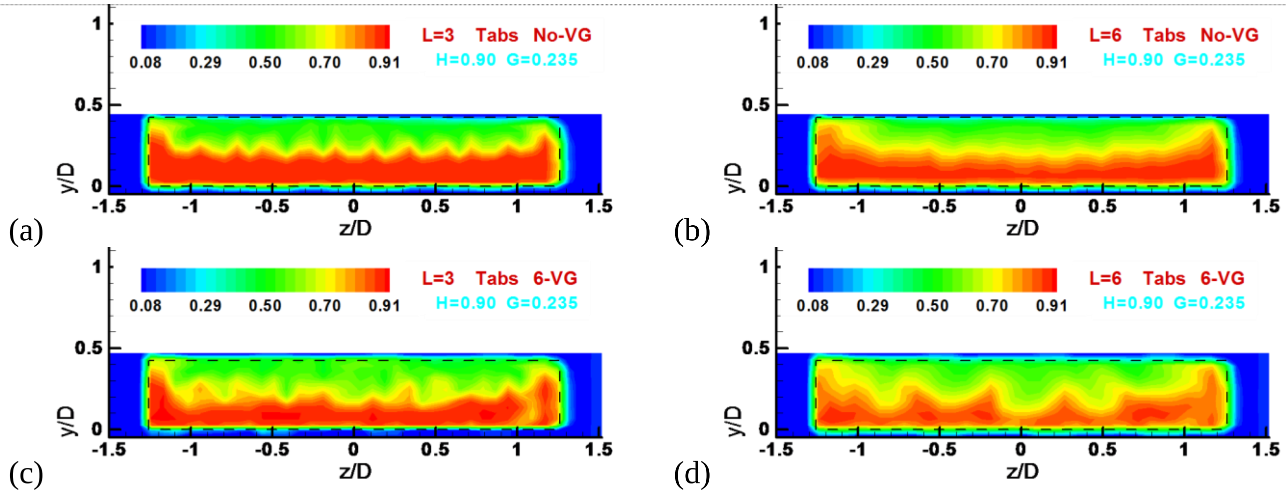

Fig. 11 Mach number contours at exit of one-sided ejector (x=0.240”) with and without 6 VG’s on the floor; M_j =0.9. Data are for two ejector lengths ($L=L_0+\Delta L$, Fig. 1a).

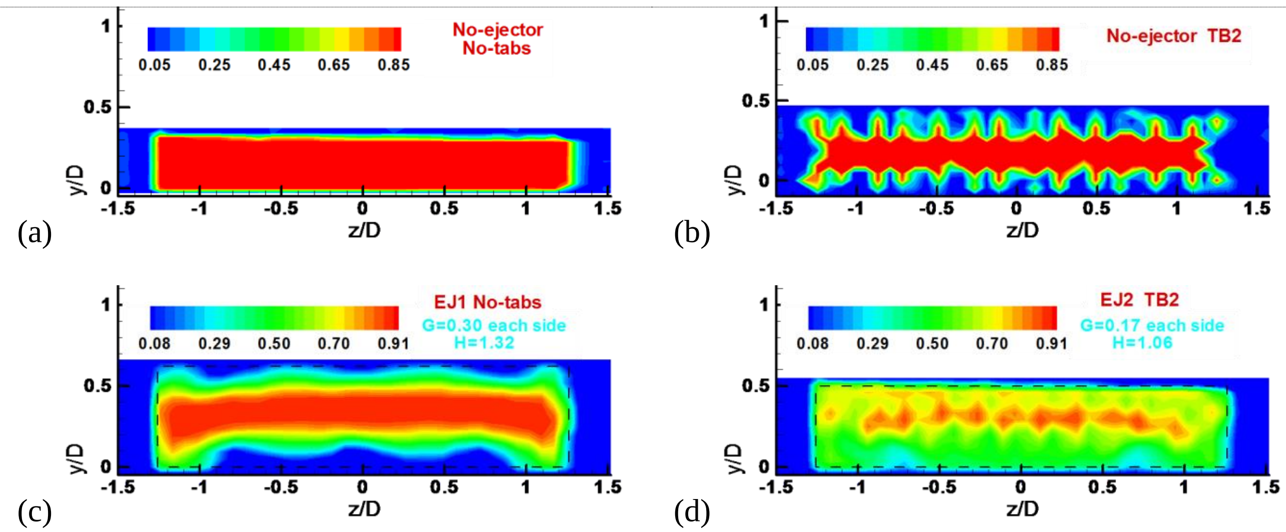

Fig. 12 Two-sided ejector. Mach number contours at exit; M_j =0.9. (a) 8:1 rectangular nozzle only, (b) Nozzle with tab configuration 2, no ejector, (c) Ejector 1, G≈0.3” on either side, no-tabs; (d) Ejector 2, G≈0.17” on lower side and G≈0.175” on upper side, with tabs.

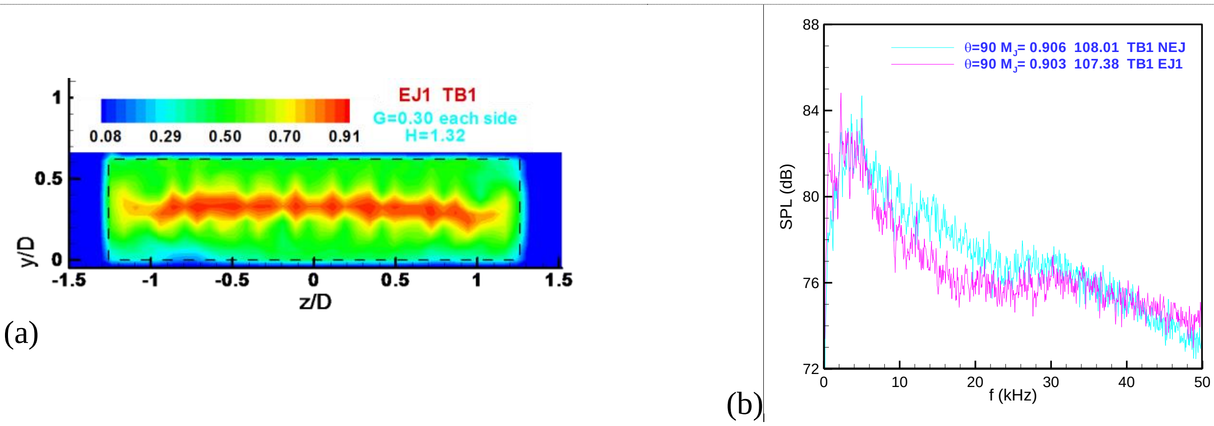

(a)

(b)

Fig. 13 Two-sided ejector with approximately 0.3” gap on either side (EJ1), tabs on upper and lower lip of nozzle have approximately 20 degree penetration (TB1). (a) Mach number contours at exit (x=0.040”), (b) SPL spectra with and without ejector; M_j =0.9.

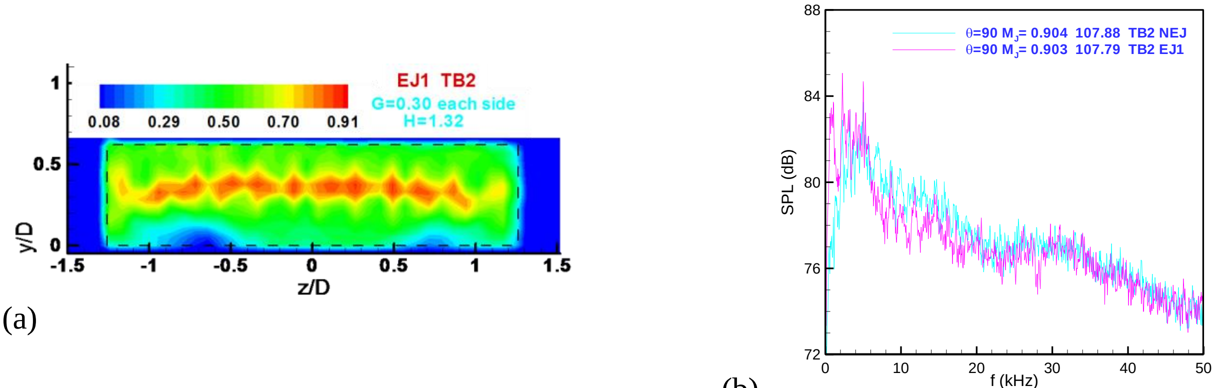

(a)

(b)

Fig. 14 Two-sided ejector (EJ1), tabs on upper and lower lip of nozzle have approximately 30 degree penetration (TB2). (a) Mach number contours at exit (x=0.040”), (b) SPL spectra with and without ejector; M_j =0.9.

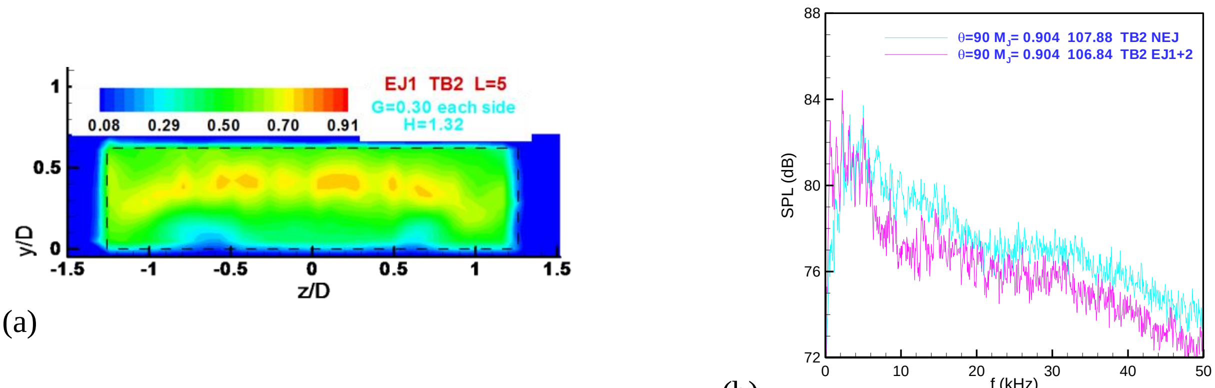

(a)

(b)

Fig. 15 Two-sided ejector (EJ1), tabs with approximately 30 degree penetration (TB2). Extended ejector length, $L=L_0+\Delta L$= 5”. (a) Mach number contours at exit (x=0.240”), (b) SPL spectra with and without ejector; M_j =0.9.

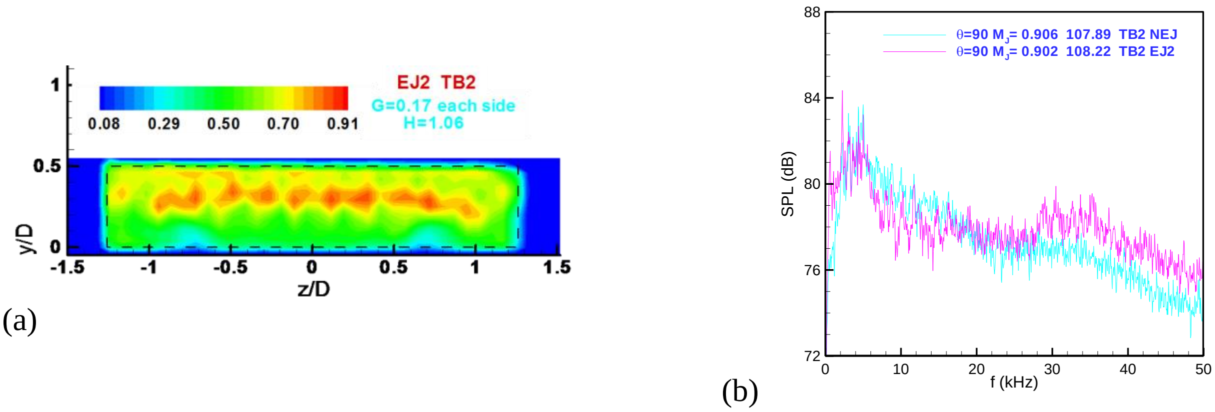

Fig. 16 Two-sided ejector with G≈0.17” on lower side and G≈0.175” on upper side (EJ2), tabs with approximately 30 degree penetration (TB2). (a) Mach number contours at exit (x=0.040”), (b) SPL spectra with and without ejector; M_j =0.9.

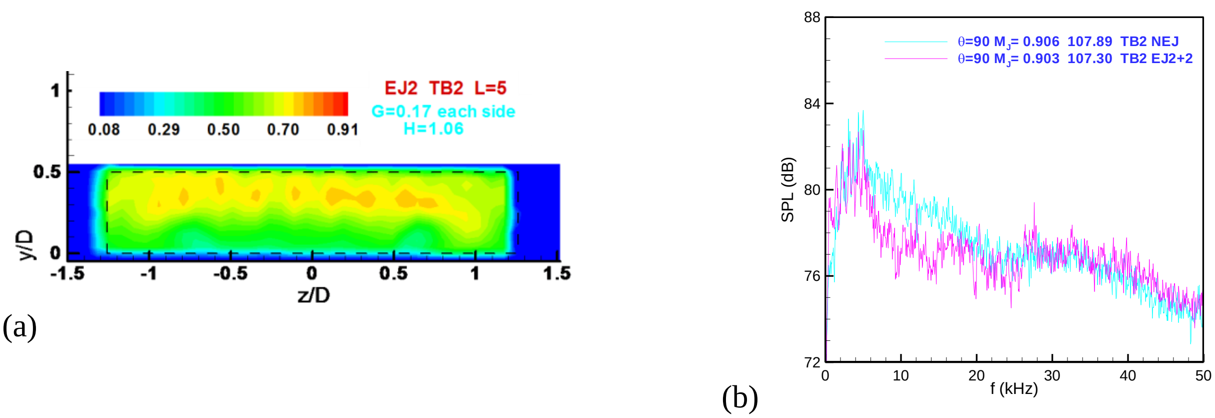

Fig. 17 Two-sided ejector (EJ2) and tabs with approximately 30 degree penetration (TB2). Extended ejector length, $L=L_0+\Delta L$= 5”. (a) Mach number contours at exit (x=0.240”), (b) SPL spectra with and without ejector; M_j =0.9.